Journal of Nuclear Materials 390–391 (2009) 160–163

Contents lists available at ScienceDirect

Journal of Nuclear Materials

journal homepage: www.elsevier.com/locate/jnucmat

Characterization of chemical sputtering using the Mark II DiMES porous plug injector in attached and semi-detached divertor plasmas of DIII-D

A.G. McLean [a,*], J.W. Davis [a], P.C. Stangeby [a], S.L. Allen [b], J.A. Boedo [c], B.D. Bray [d], S. Brezinsek [e], N.H. Brooks [d], M.E. Fenstermacher [b], M. Groth [b], A.A. Haasz [a], E.M. Hollmann [c], R.C. Isler [f], C.J. Lasnier [b], Y. Mu [a], T.W. Petrie [d], D.L. Rudakov [c], J.G. Watkins [g], W.P. West [d], D.G. Whyte [h], C.P.C. Wong [d]

[a] University of Toronto Institute for Aerospace Studies, 4925 Dufferin Street, Toronto, Ontario, Canada M3H 5T6
[b] Lawrence Livermore National Laboratory, Livermore, CA 94550, USA
[c] University of California, San Diego, La Jolla, CA 92093, USA
[d] General Atomics, P.O. Box 85608, San Diego, CA 92186-5608, USA
[e] Institut fuer Plasmaphysik Forschungszentrum, Juelich GmbH 52425, Juelich, Germany
[f] Oak Ridge National Laboratory, Oak Ridge, TN 37831, USA
[g] Sandia National Laboratories, Albuquerque, NM 87185, USA
[h] MIT Plasma Science and Fusion Center, Cambridge, MA 02139, USA

ARTICLE INFO

PACS:
28.52.Fa
44.00.00
44.30.+v
52.40.Hf

ABSTRACT

An improved, self-contained gas injection system for the divertor material evaluation system (DiMES) on DIII-D has been employed for *in situ* study of chemical erosion in the tokamak divertor environment. To minimize perturbation to local plasma, the Mark II porous plug injector (PPI) releases methane through a porous graphite surface at the outer strike point at a rate precisely controlled by a micro-orifice flow restrictor to be approximately equal as that predicted for intrinsic chemical sputtering. Effective photon efficiencies resulting from CH_4 are found to be 58 ± 12 in an attached divertor ($n_e \sim 1.5 \times 10^{13}/cm^3$, $T_e \sim 25$ eV, $T_{surf} \sim 450$ K), and 94 ± 20 in a semi-detached cold divertor ($n_e \sim 6.0 \times 10^{13}/cm^3$, $T_e \sim 2$–3 eV, $T_{surf} \sim 350$ K). These values are significantly more than previous measurements in similar plasma conditions, indicating the importance of the injection rate and local re-erosion for the integrity of this analysis. The contribution of chemical versus physical sputtering to the source of C^+ at the target is assessed through simultaneous measurement of CII line, and CD plus CH-band emissions during release of CH_4 from the PPI, then compared with that seen in intrinsic sputtering.

1. Introduction

Since chemical sputtering plays a key role in tritium co-deposition, target lifetime, and flake and dust formation, characterizing it in present day fusion devices is crucial for the successful operation of ITER [1]. In order to relate measured photon fluxes from chemical sputtering (CS) to particle fluxes at the measurement location, inverse photon efficiencies, i.e., dissociations (D) per detected photon [excitation (X) * branching ratio (B)], or D/XB values) must be derived for gases released by CS, usually by gas puffing experiments (see [5] for an excellent summary of past experiments). This experiment is based on a previous one at DIII-D [2], but with significant improvements in gas flow control, and diagnostic coverage. The porous plug injector (PPI) was built for the DIII-D divertor materials interaction (DiMES) system as an *in-situ* diagnostic to admit methane (or another hydrocarbon) through a porous graphite surface, such that its interaction with plasma and surface closely approximates a hydrocarbon molecule released from a carbon surface by CS. CH_4 is used for PPI injections as a proxy for C_xD_y released by CS in order to take advantage of the 0.5 nm separation of bandheads between CH and CD near 430 nm. Injecting methane at a known and controlled rate provides direct comparison to intrinsic emission levels for calibration of spectroscopic signals. The porous portion of the plasma-facing surface is 3.0 cm in diameter and designed such that the size and spacing of the holes is on the order of the mean free path of CH_4 in the divertor plasma. In contrast to previous measurements of D/XB which typically inject C_xH_y at rates much greater than (>10×) the intrinsic release rate of C by chemical erosion, the injection rate selected for the PPI corresponds to a 2% intrinsic $D \rightarrow C$ erosion yield, Y^{C}_{chem}, with $\Gamma_{D^+} \approx 3 \times 10^{18}/cm^2s$ [3], thus providing $\sim 4 \times 10^{17}$ CH_4 molecules/s (0.013 TorrL/s, ∼1 sccm). Additionally, the injection is not made through a tube protruding into the plasma or from between tile gaps as has been typically done in previous measurements, but in a way that mimics release of C by intrinsic chemical erosion,

* Corresponding author.
E-mail address: adam.mclean@utoronto.ca (A.G. McLean).

0022-3115/$ - see front matter © 2009 Elsevier B.V. All rights reserved.
doi:10.1016/j.jnucmat.2009.01.157

distributed over the holed area of the PPI cap at the outer strike point (OSP) (i.e., an injection flux density of $\sim 5.7 \times 10^{16}$ CH_4/cm^2/s). Emissions in excess of intrinsic background from the region above and around the PPI in the lower divertor floor are studied in typical attached and cold divertor operating regimes in DIII-D, and effective D/XB values calculated for those conditions.

2. Experiment and observations

The PPI is composed of a DiMES sample inserted flush to the lower divertor floor (within 0.3 mm), and a self-contained gas delivery system enclosed within the DiMES hydraulic arm assembly. Instead of a programmable valve which led to gas flow rates typically ~5–10× higher than desired in the previous experiment, the Mark II PPI incorporates a demountable micro-orifice flow restrictor (4.14 μm diameter) and a high pressure canister. The micro-orifice ensured that gas leaked out at a predictable and controlled rate over the course of an experimental day. New and improved diagnostic capabilities were also available for the 2007 PPI experiment. These included a new camera and optics for the multichord divertor spectrometer (MDS) which monitors emission from the PPI on a 2.1 cm diameter view-chord (the on-DiMES chord), and intrinsic emission from the graphite surface on a toroidally displaced view-chord (the off-DiMES chord). The MDS system sensitivity viewing the 430 nm region was improved by a factor of ~100 compared to 2005. A new DiMES TV camera was also installed to quantify spectral emissions both from intrinsic sources (i.e., for background subtraction) and from the PPI puff away from the DiMES region (i.e., to quantify emission away from the MDS on-DiMES chord) in the lower divertor region (Fig. 1).

An L-mode deuterium plasma with a lower single-null (LSN) shape was developed with parameters of $I_p = 1.1$ MA, $B = 2.0$ T, $P_{NBI} \sim 0.23$ MW, $\langle n_e \rangle \sim 2.5 \times 10^{13}$ cm^{-3} in attachment and $\langle n_e \rangle \sim 5.0 \times 10^{13}$ cm^{-3} in detachment. Shots were run with the OSP swept over divertor shelf and held steady at the inboard edge of the DiMES port ($1.462 < R_{DiMES} < 1.510$ m). The OSP above the PPI had a region where n_e and T_e were >90% of their peak values which was ~5 cm in radial extent. Langmuir probes, and divertor Thomson scattering (DTS) provided plasma parameters, and filterscopes provided additional data on hydrogenic and intrinsic impurities near the target. OSP plasma parameters were as follows: In attachment, $\Gamma^{\parallel}_{D^+,att} \sim 3.0 \times 10^{18}/cm^2/s$, $n_e \sim 1.5 \times 10^{13}/cm^3$ and $T_e \sim 25$ eV, and in a semi-detached cold divertor, $\Gamma^{\parallel}_{D^+,det} \sim 6.5 \times 10^{18}/cm^2/s$, $n_e \sim 6.0 \times 10^{13}/cm^3$ and $T_e \sim 2$–3 eV. The ratio of D_β/D_α emission from attached to cold divertor operation was found to rise from ~0.1 to ~0.2, while integrated $D\gamma$ emission, ϕ_{D_γ}, rose by ~20×, confirming a low divertor temperature, but indicating that the plasma did not fully detach at the target in the transition from attached operation. This is confirmed by the ion saturation current measured by Langmuir probes which stays approximately constant through most of the increase in $D\gamma$ emission before eventually falling (i.e., roll-over). Surface temperature at the target was measured by infrared camera to be $T_{surf} \sim 450$ K in attachment, and $T_{surf} \sim 350$ K in the cold divertor.

Sample spectra from the MDS ($\Delta\lambda = 0.00765$ nm, $\lambda/d\lambda = 56{,}300$, 7.8 nm spectral range, 200–250 ms integration time) are shown in Fig. 2 for attached plasma conditions. Spectrally integrated emission from the gas puff (i.e., incremental emission over the intrinsic signal, due to the puff-only) is determined by subtracting the signal off-DiMES from the signal on-DiMES. Emission from the puff is found to be approximately equal in strength to that from intrinsic sputtering in both plasma conditions. Integrated puff-only CD plus CH emission, $\phi^{\text{puff-only}}_{CD+CH}$, versus PPI flow rate shows a highly linear relationship over the puffing rates in both attached and cold divertor plasmas, indicating that perturbation to the local plasma was minimized. The intensity of H_γ (434.2 nm) as a consequence of the PPI puff was found to be equivalent to ~2–3% of the local D_γ (433.9 nm) emission at the DiMES location in attachment, indicating the puff had a minimal impact on local hydrogenic recycling

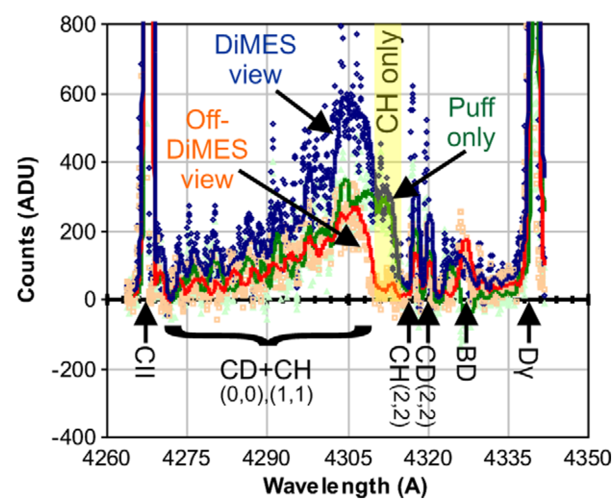

Fig. 2. Spectral profiles of the CD- and CH-band region from the MDS diagnostic in attached divertor plasma, showing the emission at the PPI (blue), the intrinsic emission away from the PPI (red), and the difference due to the puff alone (green). Profiles with similar intensities and structure are found in cold divertor conditions. (For interpretation of the references to colour in this figure legend, the reader is referred to the web version of this article.)

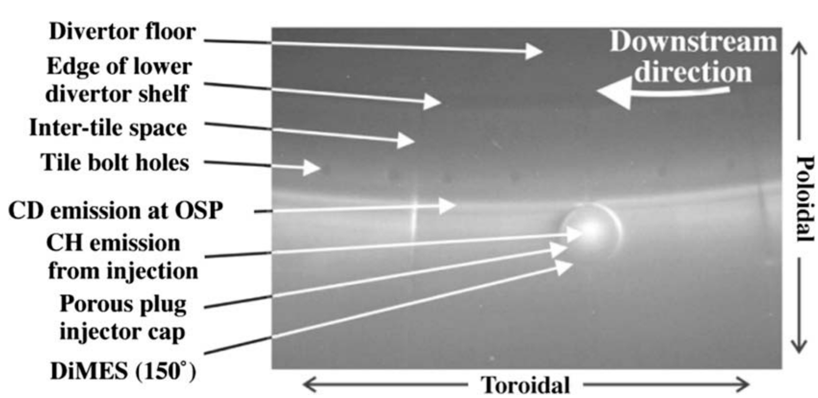

Fig. 1. Image from DiMES TV viewing a 50 × 60 cm extent of the lower divertor in DIII-D. A CD and CH filter is used (centre: 430.5 nm, bandpass: 3.5 nm), showing emission from the OSP and SOL, and that from the PPI above the intrinsic background.

in that condition. Boron is a significant impurity in DIII-D due to the boronization (BZN) process used for wall conditioning. The boron deuteride (BD) A-X band emits in the 430 nm region [4]; the p-branch overlaps the CD and CH A-X band in the 427–432 nm region, while the q-branch is more isolated from CD and CH in the region of 432.5–432.8 nm. Through correlation of the integrated intensity of each BD branch immediately following a BZN on DIII-D when CD emission was minimal, the contamination of CD and CH in the 427.0–431.5 nm region by the BD-band was determined and led to a 10–50% correction in the PPI data.

3. Discussion

The effective D/XB for CH includes consideration for all breakup, prompt deposition, and re-erosion processes that 'pass through' the CH molecular fragment. For CH and CD, a full account of emission in the A-X Gerö band is made using a 'full span' expansion factor [5], $f^{CH\,or\,CD}_{A-X}(T_{rot}\sim 0.3\text{ eV}, \lambda_{span}) = 1.8$, λ_{span} = 427.0–431.5 nm. The effective D/XB values for CH are calculated as

$$\left[\frac{D}{XB}\right]^{CH_4\to CH}_{A^2\Delta\to X^2\Pi} = \frac{\Gamma^{CH_4}}{\phi^{CH_4\to CH}_{A^2\Delta\to X^2\Pi}\cdot f^{CH}_{A-X}(T_{rot},\lambda_{span})}, \quad (1)$$

and equal to 58 ± 12 in attachment, 94 ± 20 in the cold divertor. These values are somewhat higher than those derived in the 2005 experiment. They are, however, in contrast to the only other data which is taken at an injection rate on the order of the intrinsic CS rate [4] in which $\Gamma^{CD_4} = 5\times 10^{17}$/s were injected from an inlet extended into the SOL. The observation that the current values and those of [4] are so far outside the error bars for previous measurements may be because processes involved at injection rates equal to intrinsic CS rates differ from those at the higher ($\geqslant 10\times$ intrinsic) rates which were used for all other measurements reported, including those of the 2005 PPI experiment (i.e., perturbation of local plasma conditions is significant at higher injection flux densities). The inverse photon efficiency for CH is found to increase by a factor of ~2 from attachment to the cold divertor which is in agreement with observations made in the 2005 experiment and other data previously reported [2].

The average chemical erosion yield over the MDS view chord at the OSP may be deduced by comparison of the integrated emission from intrinsic sources with that from the PPI for a known injection rate, by the relation

$$Y^{C}_{chem} = \frac{\Gamma_{CH_4,PPI}}{\Gamma_{D^+}}\cdot\frac{\phi^{Intrinsic}_{CD}}{\phi^{PPI\,puff}_{CH}}, \quad (2)$$

where Γ_{D^+} is the perpendicular ion flux over the holed region of the PPI as measured by the Langmuir probes. In attached conditions, a 2.6 ± 0.5% is found which is in agreement with laboratory measurements [6], but significantly higher than previous inferred measurements on DIII-D [7]. The lack of agreement to previous experiments may have been due to a high detection threshold for the MDS system which negatively impacted the ability of the spectrometer to accurately account for 430 nm CD band emission. In the cold divertor, a yield of 0.5 ± 0.3% is found, accounting for ionized hydrogenic flux alone (i.e., no accounting for neutral hydrogenic flux). While this value is approximately that expected from laboratory measurements (for $D^+ = 10$ eV $Y^{C,300K}_{chem}\approx 0.7\pm 0.2\%$, and $Y^{C,500K}_{chem}\approx 1.7\pm 0.2\%$ [8]), the CS yield in the cold divertor is not found to decline drastically as has been inferred previously on DIII-D for $T_e \leqslant 1$ eV (i.e., $Y_{chem} < 10^{-4}$). This former observation in detachment, however, may be because only a semi-detached state was achieved at the OSP.

Production efficiencies, described in [2], for CH from injection of CH_4 are found using code-calculated direct D/XB values for CH from HYDKIN [11]. Production efficiencies are found to be $\eta_{CH_4\to CH,att} = \Gamma_{CH}/\Gamma_{CH_4} = 0.75\pm 0.1$ into attached divertor conditions, and $\eta_{CH_4\to CH,det} = \Gamma_{CH}/\Gamma_{CH_4} = 0.08\pm 0.01$ from injection of CH_4 into cold divertor conditions. These values are higher than those measured in the 2005 PPI experiment with a 10× higher gas puff rate, possibly due to self-shielding of CH_4 from the local plasma in the previous experiment which would lead to lower interaction than occurs at intrinsic levels. This difference may highlight a necessity to utilize a C injection rate in the puff on the order of the intrinsic C-release rate due to CS in order to accurately characterize intrinsic sputtering processes.

For these experiments, the PPI gas puff imitates a source of purely chemically eroded carbon, and thus the resulting ratio of CII to CH and CD emission for the puff can be considered indicative of the intrinsic CS source. The ratio of the spectrally integrated CD and CH-band brightness (427.0–431.5 nm) to that of the nearby CII line (426.7 nm) provides, in principle, a direct method for determining the relative contribution to the C^+ source by CS versus that of other sources, primarily physical sputtering. In Fig. 3, the relationship between φ_{CII} (426.6–426.85 nm) and φ_{CD} (427–431 nm, with BD-band correction) is shown for intrinsic sources at the OSP, and found to be linear. Spectrally integrated data for the puff alone is shown in Fig. 4 and also found to be linear, further indicating that the puff was non-perturbative to the local plasma. These data demonstrate that the magnitude of integrated CD and CH from the puff is approximately equal to that of the intrinsic data, indicating that the puff was effective at replicating CD emission from intrinsic chemical erosion. The slope of the linear fit to the puff-only data in attached plasma, Fig. 4(a), is ~50% of that for the intrinsic emission leading to the conclusion that sources of C^+ produced by CS contribute about ½ of the total in attached divertor conditions. This conclusion is contrary to observations made for C^0 sources based on the CI line profile [9], is in agreement with PPI data analyzed at CI (910 nm), and CII (514 and 658 nm) where a C^0/C^+ contribution from CS of 10–20% is measured. These data are the focus of ongoing study and modelling using a 3-D version of the DIVIMP-HC Monte Carlo code by Mu et al. [10]. Fig. 4(b) shows the puff-only data in the cold divertor where the puff contributes very little to measured CII emission, and is therefore inferred to be a minor, ~10%, contributor to local C^+ at the OSP. Intrinsic CII in the cold divertor may be primarily from recombination of carbon in higher charge states transported from the

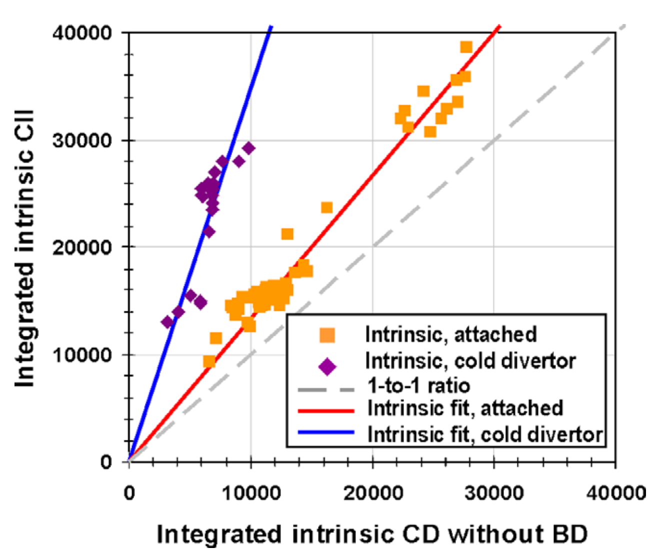

Fig. 3. Spectrally integrated CII line (426.7 nm) versus CD band (427–431 nm) emission is shown for the intrinsic chemical sputtering source near the OSP in shots with steady attached and cold divertor conditions.

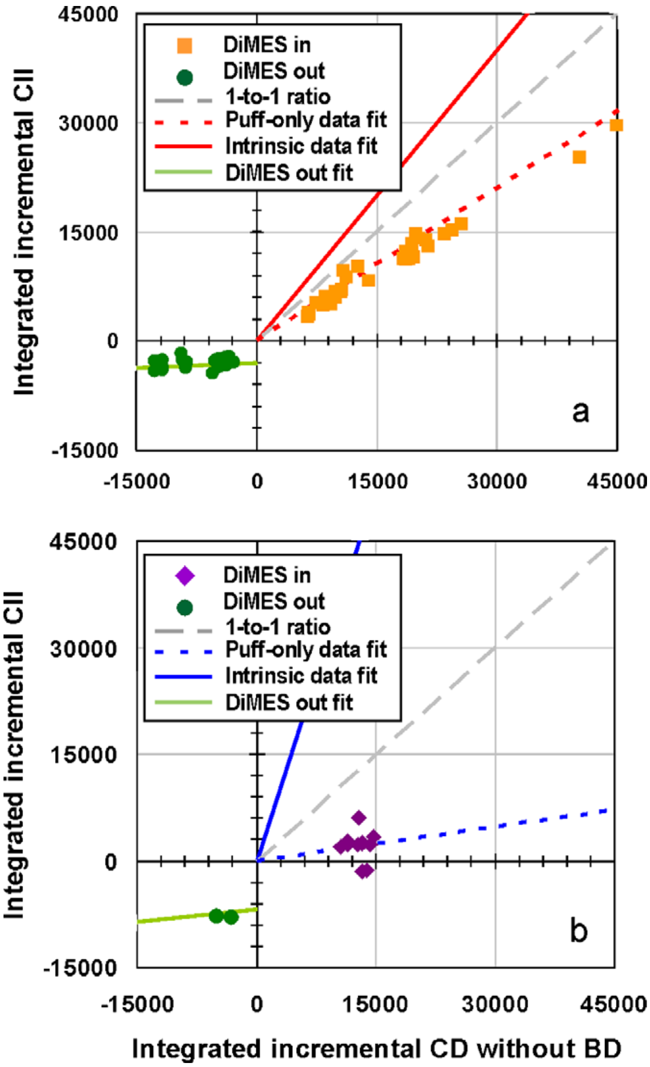

Fig. 4. Incremental integrated CII versus CD and CH for emission from the PPI gas puff-only in shots with (a) a steady attached divertor, and (b) a steady semi-detached divertor. In attachment, data from the puff alone is fit to a linear slope of ∼0.8. In the cold divertor, incremental integrated CD and CH is found to be larger than that of CII by a factor of ∼10:1, indicating that CS is a minor contributor to C^+ near the OSP at this plasma condition.

scrape-off layer (SOL). Emission of CH and CD in the cold divertor does not extinguish as previously observed at the OSP with $T_e \leqslant 1$ eV [7]. When DiMES is recessed and a blank hole left in the attached divertor surface, reductions of 15–20% in the CII emission and 30–55% of the CD emission are found compared with the intrinsic emission with a graphite surface present. In cold divertor conditions, reductions of 25–30% of the intrinsic CII emission and ∼50% of the intrinsic CD emission are found. These observations highlight the need to determine the source of the emissions that remain when the local surface is removed in both conditions.

4. Conclusions

The Mark II DiMES PPI has been successfully utilized for detailed characterization of erosion processes at the OSP of L-mode attached and cold divertor plasmas in the DIII-D divertor. Direct comparison between intrinsic emission of CII and CD as a consequence of sputtering processes near the OSP, and those of a localized, controlled artificial injection of CH_4 through a porous cap closely imitating a solid graphite surface have been reported. Integrated emission of CH resulting from the gas puff was found to approximately equal that of intrinsic CD. An inferred contribution of chemical sputtering to C^+ near the OSP based on the intensity of the CH and CII (426.6–426.85 nm) emission cloud from the puff has been found to be ∼50% in attached conditions and only ∼10% in cold divertor conditions, but is not supported by other C-line emissions, CI (910 nm) and CII (514 and 658 nm), which indicate a C^0/C^+ contribution from chemical sputtering of 10–20%. Resolution of this difference is the focus of ongoing 3D modelling. Effective inverse photon efficiencies D/XB and production efficiencies η for CH have been reported. The intrinsic chemical erosion yield near the OSP has been inferred to be 2.6 ± 0.5% in an attached divertor, and 0.5 ± 0.3% in a cold divertor plasma.

Acknowledgments

The authors would like to acknowledge the support of a Collaborative Research Opportunities Grant from the Natural Sciences and Engineering Research Council of Canada and the US Department of Energy. This work supported by the U.S. Department of Energy under DE-FC02-04ER54698, DE-FG02-04ER54762, DE-AC52-07NA27344, DE-FG02-07ER54917, DE-AC05-00OR22725, DE-AC04-94AL85000.

References

[1] A. Loarte et al., Nucl. Fusion 47 (2007) S203.
[2] A.G. McLean et al., J. Nucl. Mater. 363–365 (2007) 86.
[3] P.C. Stangeby et al., J. Nucl. Mater. 313–316 (2003) 883.
[4] S. Brezinsek et al., Phys. Scripta T128 (2007) 40.
[5] S. Brezinsek et al., Phys. Scripta T111 (2004) 42.
[6] J.W. Davis, A.A. Haasz, J. Nucl. Mater. 241–243 (1997) 37.
[7] D.G. Whyte et al., Phys. Scripta T111 (2004) 34.
[8] G.M. Wright et al., J. Nucl. Mater. 337–339 (2005) 74.
[9] N.H. Brooks et al., J. Nucl. Mater. 363–365 (2007) 131.
[10] Y. Mu et al., J. Nucl. Mater. 390–391 (2009) 220.
[11] D. Reiter (2006) http://www.eirene.de.